THE JOURNAL OF PHYSICAL CHEMISTRY B

Article

pubs.acs.org/JPCB

Role of Water in the Formation of the Electric Double Layer of Micelles

Elena Brodskaya

Department of Chemistry, Saint Petersburg State University, Saint Petersburg, Russia

ABSTRACT: The surface layer of a direct ionic micelle with explicit solvent was simulated by the molecular dynamics method. Local properties of the system were calculated in the spherical micellar cell. The results for the local electric potential show that the contribution of a polar solvent makes the potential short-ranged, in contrast to predictions of the Poisson−Boltzmann theory.

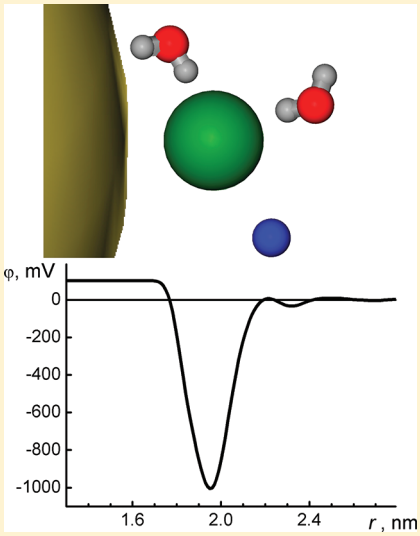

I. INTRODUCTION

The electrical double layer (EDL) around ionic micelles arises because of the spatial charge separation in micellar solutions as it occurs in any colloidal systems.[1] Various theoretical approaches to description of local electric properties of the EDL around a colloid particle are mostly based on the Poisson−Boltzmann approximation or integral equations for the distribution functions. The solvent in these approaches is usually considered as a continuous medium with a constant value of the dielectric permittivity. The classical computer simulation methods, Monte Carlo (MC) and molecular dynamics (MD),[2,3] can provide "experimental" bases for these theories.

One of the first simulations of the EDL near a charged surface by MC method was done in the work by Torrie et al.[2] At present, there are numerous papers on simulation of electric double layers near flat,[4−12,19] cylindrical,[13−15] and spherical[16−18] surfaces within the framework of the continuous solvent model. However, the results of these simulations are rather contradictory. While for one−one electrolyte solutions and moderate field strength a reasonable agreement between the theories and simulations can be achieved, a considerable difference is observed for solutions with higher valency ions or stronger external field.[15] In refs 17 and 18 the authors conclude that "the widely used PB theory is found to have important quantitative and qualitative disagreements with the MC results". In ref 19 it was found that taking into account a local concentration approximation improves the agreement between the simulations and the mean-field Poisson−Boltzmann equation. The disagreements between the theory and simulations stem mainly from neglecting of the local contribution of the polar solvent to the formation of an EDL. Therefore, the attempts to solve the problem were undertaken by the introduction of an empirical-based local dependence of the dielectric permittivity of the solvent (see e.g. ref 20). The influence of the molecular character of the solvent on EDL properties was taken into account in the simulations reported in refs 21 and 22 In ref 21 the solvent molecules in the surface layer near the charged plane were modeled as hard spheres. Nonmonotonic local charge and solvent distributions due to steric interactions were obtained that are not consistent with the PB mean-field approximation. For local electric properties around the spherical macroion, a coarse-grained description of water was compared with the implicit solvent model in the paper.[22] No qualitative difference in charge distribution was found for the two solvent models.

Obviously, the polar character of a solvent should appreciably affect EDL properties near charged surfaces. In the first works with an aqueous electrolyte solution represented using the explicit solvent model, the solution was simulated near a charged plane solid surface,[23−29] and multilayer ion and water distributions were obtained. A similar behavior was observed in MD simulations of a surfactant monolayer on the water/carbon tetrachloride interface.[30] The difference for local charge profiles

Received: March 13, 2012
Revised: April 20, 2012
Published: April 30, 2012

dx.doi.org/10.1021/jp3024183 | J. Phys. Chem. B 2012, 116, 5795−5800

was revealed for anionic (sodium dodecyl sulfate) and cationic surfactants.

Quite numerous works reported simulations of micellar solutions using different levels of presentation of the solvent (see e.g. reviews in refs 31 and 32). However, local behavior of the electric potential almost was not discussed previously. A substantial disagreement with the PB mean-field approach was observed in the case of discrete micellar charges and a rough micellar surface.[33,34] In the simulations,[35] local electric potential was calculated near the micelles of zwitterionic surfactant (DPC), and an appreciable compensation effect of water was first registered. In the review,[36] the influence of water on the local charge structure near cylindrical polyions (biomolecules, DAN molecules, proteins, etc), which could not be explained by the PB theory, was also described. The main finding of these studies is a nonmonotonic behavior of the counterion density around macroions or micelles.

The main objective of the present paper is to perform a molecular dynamics study of the local distribution of species near a spherical micelle and to analyze the local electric potential using an explicit water model within the frame of the micellar cell. In the previous molecular dynamics study,[22] special attention was paid to the dependence of the local characteristics of the micellar surface layer on the molecular structure of the coarse-grained solvent. It was shown that the local potentials for continuous and coarse-grained descriptions of the solvent are similar. However, there is a striking difference in the behavior of the local electric potential for the atomistic and coarse-grained models of the solvent. The present paper is devoted to a more detailed analysis of the local properties of the surface layer of both anionic and cationic micelles.

II. MODEL AND COMPUTATIONAL DETAILS

A spherical ionic micelle was placed in the center of a droplet of an aqueous solution of counterions. The drop contained 7500 water molecules of the SPC/E model[37] (Table 1). The whole system was confined in the spherical shell, which generates a short-range repulsion field acting upon molecules and ions. The radius of the shell was equal to 5.5 nm and was large enough to allow existence of a vapor phase between the shell and the liquid drop. So, two surface layers are formed in the system. One of them is near the micelle itself, and the second one is on the liquid/air (vacuum) boundary. As it will be shown later, both layers are independent and the existence of the liquid/air surface does not influence the structure of the solution in the vicinity of the micelle. So, a micellar system is represented as a nanodroplet with diameter equal to about 10 nm surrounded by a vapor phase. To verify whether there is an influence of the external spherical boundary upon local properties in the proximity of the micelle, we performed yet another simulation. A micelle in the liquid solution with no vapor phase was confined in the cubic cell, periodic boundary conditions being employed. Similar results have been obtained using the both types of the boundary conditions.

Table 1. Parameters of the Interaction Potentials of Components

	ε, 10^{-21} J	σ, nm	q, e
O^-	1.079	0.316	−0.8476
H^+			+0.4238
Hd	5.900	0.470	+1 or −1
Na^+	0.695	0.258	+1
Br^-	0.695	0.370	−1
CH_4	2.044	0.373	

The model of a spherical micelle is similar to the one proposed in ref 38. The ionic micelle consists of a rigid hydrocarbon core and 60 one-site ions of surfactant (SAS) harmonically bounded to the core. 60 counterions (Na^+ and Br^-) were distributed in the liquid drop. The specified parameters are the radius of the hydrocarbon core (1.5 nm) and coarse-grained parameters for the head ions of SAS (Hd^+ or Hd^-). The interactions between components are described as the sum of Lennard-Jones and Coulomb potentials without any limitations on the long-range forces. It is an important feature because in the case of a finite action range of the interactions, a nonrealistic condensation of ions of the same charge is observed. The parameters for the counterion Na^+ were taken from the work[39] (Table 1).The Lennard-Jones parameters for the anionic and cationic micelles are the same. The interaction of the core with the components is calculated analytically by integration of the Lennard-Jones potential over the sphere with a hydrocarbon liquid density. The parameters of CH_4 were used to describe the molecules of hydrocarbon core[40] (Table 1).

The micellar crown is permeable to the species present in the solution. These model micelles can be considered as quite rough representations of sodium dodecyl sulfate and cetyltrimethylammonium bromide micelles. The model used here is quite simplified in comparison to the previous works[41] where all the components including the SAS molecules were described atomistically. Nevertheless, the model allows one to determine the local electric field with minimal distortions due to the micelle shape fluctuations. Except this, the exclusion of the process of micelle formation accelerates equilibration of the system during MD simulations and considerably facilitates collecting the equilibrated data. An additional argument in favor of the model is that water does not penetrate into the micelle core.[42−44]

The temperature was kept equal to 300 K by employing the Berendsen thermostat. The systems are observed for no less than 10 ns. The local characteristics of interest include local partial densities of components, $\rho_i(r)$; density of the electric charge, $\rho_q(r)$; local electric potential, $\varphi(r)$; the orientation distribution functions for water molecules. The orientation of the dipole moments, OH, and HH bonds was characterized by the angle between these vectors and the radius vector of the oxygen atom in a molecule.

The equations for local electric potential were proposed in the works[45,46] for pure water clusters:

$$\varphi(r) = \frac{1}{4\pi\varepsilon_0}\left\langle \sum_{i,(r<r_i)} \frac{q_i}{r_i} + \sum_{i,(r>r_i)} \frac{q_i}{r} \right\rangle$$

Here ε_0 is the dielectric constant of vacuum and q_i is the point charge of an ion or atom. The angle brackets identify averaging over time.

III. RESULTS AND DISCUSSION

Local Structure. The local partial densities of species around the micelles are shown in Figures 1 and 2. The distributions of micellar ions and counterions are fairly similar for the anionic and cationic micelles. They are characterized by narrow symmetric density profiles for head ions with the

dx.doi.org/10.1021/jp3024183 | J. Phys. Chem. B 2012, 116, 5795−5800

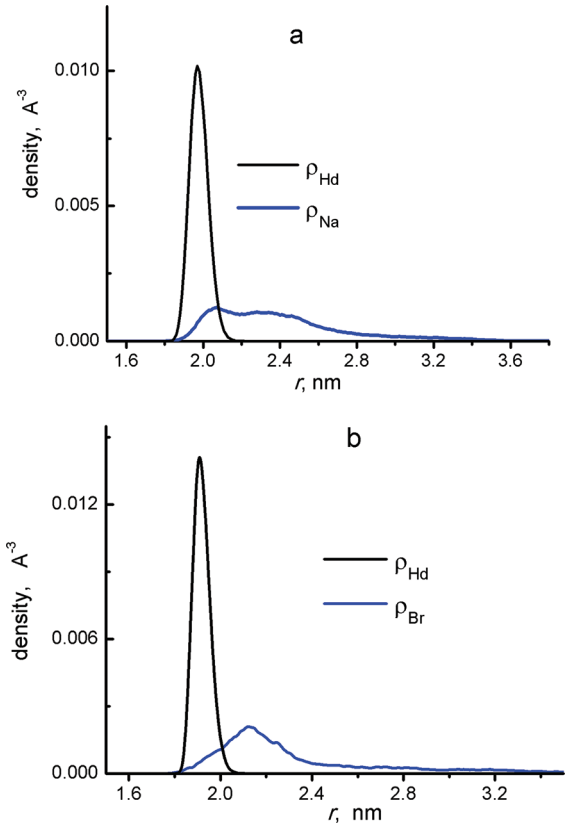

Figure 1. Local density profiles of head ions and counterions around the anionic (a) and cationic (b) micelles.

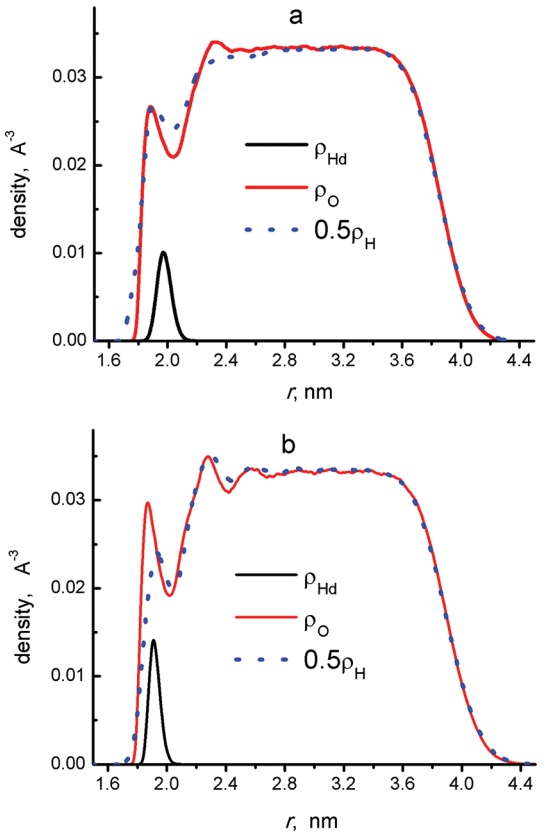

Figure 2. Local density profiles of water atoms (oxygen and hydrogen) and head ions around the anionic (a) and cationic (b) micelles.

maxima at 1.96 nm for Hd^- and 1.91 nm for Hd^+ (Figure 1). This region constitutes the so-called micellar crown. Some difference can be seen in the counterion distributions for the two micelles. The function for counterions near the cationic micelle has one maximum shifted from the micellar crown to a distance of ∼2.13 nm so that Br^- ions are predominantly located outside the headgroup region. Although Na^+ ions around the anionic micelle could be closer to the head groups, their density has a smooth maximum shifted to 2.04 nm. At higher distances, the density of Na^+ is almost constant until about 2.5 nm and then monotonically drops to zero near 3.5 nm.

In Figure 2, the hydrogen atom density divided by two is presented, along with the densities of the head ions and of oxygen atoms, to make the picture easier to understand. According to the distributions of oxygen and hydrogen, two surface layers can be seen in the systems. One of them is near the micelle itself, and the second one is the external surface layer on the boundary with the vapor (vacuum). It is worth mentioning that in a rather large region of the system (2.7 nm < r < 3.7 nm) the total density appears to be almost constant. This region will hereafter be referred to as the "bulk". This allows us to suppose that the electric double layer is unaffected by the external shell of the simulation cell.

One can see that water molecules penetrate into the micellar crown up to the contact with the hydrophobic core. The first maximum in the density profiles contains the molecules forming the hydration shells of the head ions. It is possible to estimate the hydration number of a micelle by integrating over this layer. For the anionic micelle, the mean value of the hydration number per one head ion is equal to 5.4, in accordance with the data from the work.[40] This fact confirms the validity of the simplified description of the head ions in this model. Around the anionic micelle, the peaks for both atomic densities are located practically at the same point.

For the cationic micelle, the oxygen atom distribution is slightly more structured in the vicinity of the head groups (Figure 2b). As a consequence, the hydration shell of the head groups contains a larger number of water molecules per a group (∼7.6). The hydrogen atom distribution differs from the anionic micelle considerably. The first peak of the hydrogen atom density lies slightly further from the micelle center than the peak for oxygen. Moreover, the second maximum belonging to another hydrogen atom of the same water molecule is developed much better than in the anionic micelle. In both systems, the water distribution differs significantly from the relatively homogeneous bulk over a distance range about 1.0 nm; so, the difference in oxygen and hydrogen distribution can be detected over approximately three molecular layers.

Orientation Distribution Functions. Along with the local density, the orientation distributions of water molecules depend on the distance from the micelle. In Figure 3, the orientation distribution functions of water around the anionic micelle are shown for the dipole moments (Figure 3a) and OH bonds in the vicinity of the micelle (Figure 3b).

According to Figure 3a, the dipole orientation distribution with a maximum at 110°−120° is similar for the regions near the hydrophobic core and at the boundary with vapor. The same arrangement of water molecules was also observed at the surface of pure water clusters.[46,47] In the second layer the dipole moments tend to be directed toward the center of the micelle. This orientation of dipoles, though considerably weaker, is preserved in the bulk region. In the proximity of

dx.doi.org/10.1021/jp3024183 | J. Phys. Chem. B 2012, 116, 5795−5800

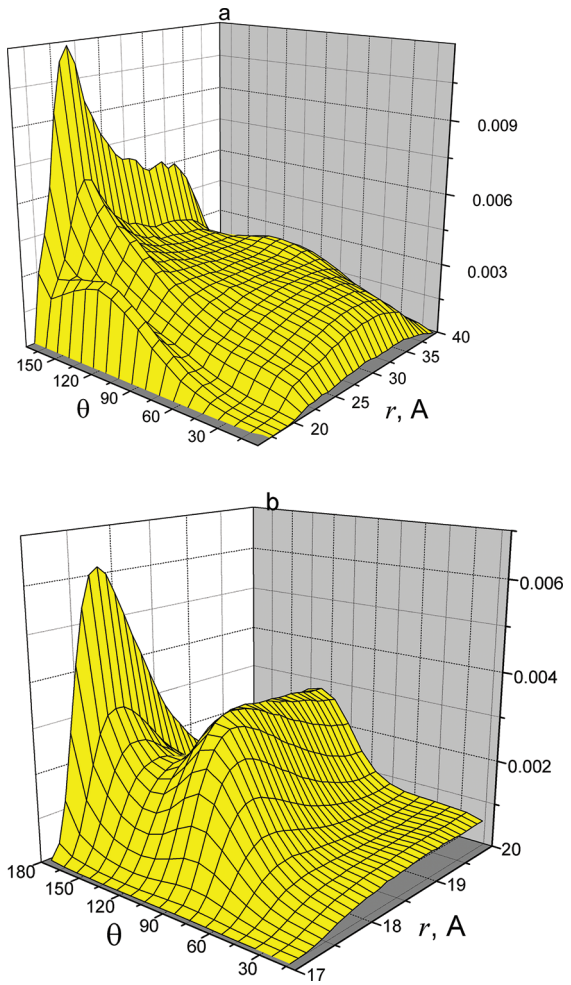

Figure 3. Orientation distribution functions for water molecules in the system with the anion micelle: (a) dipole moment distribution; (b) distribution of OH-bonds in vicinity of the micelle.

the micelle, one of the hydrogen atoms of a molecule is preferably directed to the hydrophobic core. This is clearly seen in Figure 3b where the OH-bond orientation near to the anionic micelle core is shown.

Local Electric Charge and Potential. From the local densities, it is easy to calculate the local charge distribution. The partial contributions to the total charge are shown in Figure 4. Taking into account the effective charges of water atoms, causing the dipole moment of water molecule, gives a complicated spatial dependence of the local total charge that could not be represented by the model of two oppositely charged surfaces. There are several well-developed extrema. In the case of the anionic micelle, the first maximum is due to hydrogen atoms of water penetrating into the micelle crown (Figure 2a). One of these atoms in a water molecule is directed to the micelle core. Water molecules and counterions contribute almost equally to the second maximum. Between these two maxima, there is a deep negative minimum caused by the anions of the micelle. The following small negative minimum appears due to some predominance of the contribution from oxygen atoms of water. At higher distances from the micelle center, the total charge practically cancels out at 2.4 nm and further. It means that there is no diffuse charge layer around the micelle which could be observed if the contribution of water would not be taken into account. The

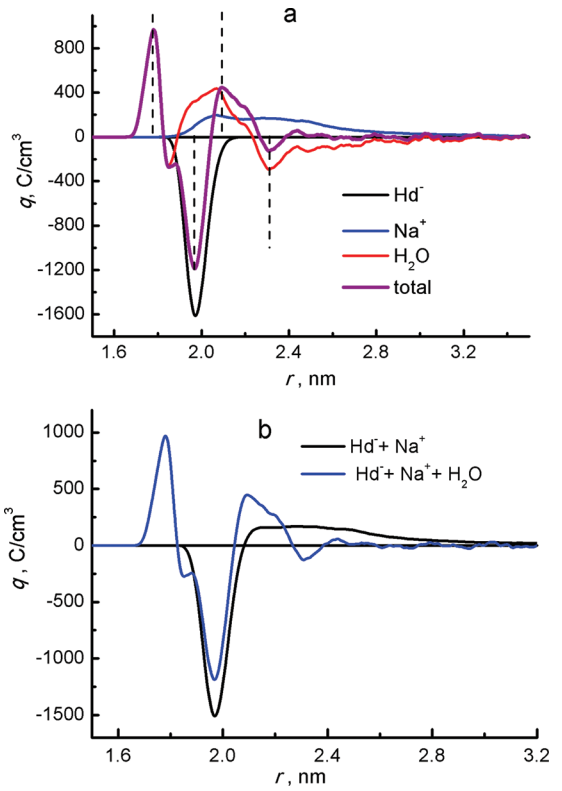

Figure 4. Local charge distributions around micelles: (a) partial contributions from components around the anionic micelle; (b) total local charge with and without the water contribution around the anionic micelle.

difference in the behavior of the local charge with and without the water contribution can be clearly seen in Figure 4b. Thus, water molecules around micelles provide different contributions to the total charge in the different regions of the system. They amplify the contribution from counterions inside the micellar crown and practically compensate it outside the crown.

A similar complicated behavior of the local charge distribution was observed in ref 30 for the monolayer of SDS at the interface between water and carbon tetrachloride. However, our results for the charge distribution around the cationic micelle shown in Figure 5 differ slightly from those obtained in ref 30. Instead of only two extrema of charge distribution, we have observed four main extrema around the cationic micelle (Figure 5). Such a discrepancy may be

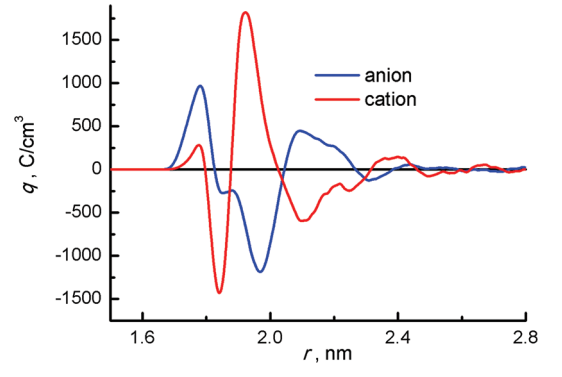

Figure 5. Local charge distributions around the anionic and cationic micelles.

dx.doi.org/10.1021/jp3024183 | J. Phys. Chem. B 2012, 116, 5795−5800

attributed to the rigid model of the hydrophobic core and the curvature of the surface layer of the micelle.

The complicated behavior of water in the system exhibits itself in the local electric potential function (Figures 6 and 7).

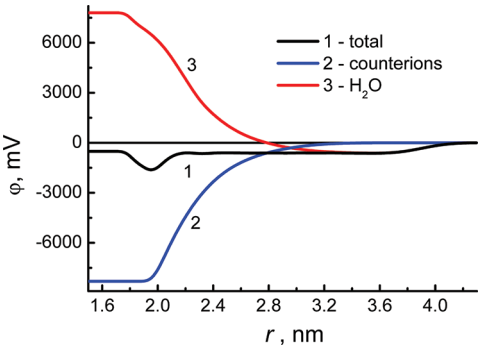

Figure 6. Local electric potential around micelles (1) and the contributions from water molecules (2) and counterions (3) around the anionic micelle.

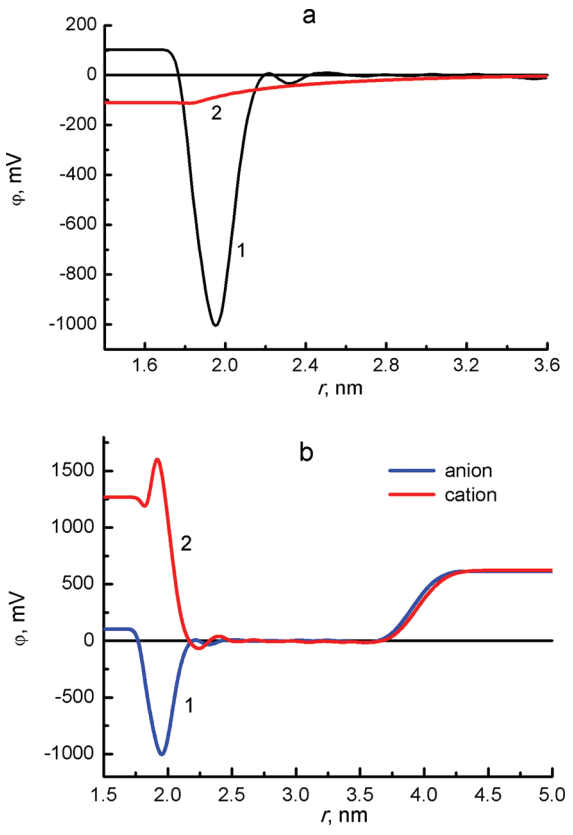

Figure 7. Local electric potential around the micelles: (a) the potential around an anionic micelle from simulations with explicit water (1) and with implicit solvent with dielectric permittivity $\varepsilon_d = 78.5$ (2); (b) the local potential in the systems with anionic (1) and cationic (2) micelles.

The contribution of counterions (Na^+) to the electric potential increases to zero monotonically until about 3.2 nm from the micelle center (Figure 6). Further from the center, the water contribution prevails over the counterion contribution. The negative mimimum of the potential near 1.95 nm originates from the head anions. In the 2.2 nm < r < 3.8 nm region, Figure 6 shows an almost constant value of the total potential which is close to the value for the bulk water, about −0.5 to −0.6 V.[45,46,48] That means that the surface potential of the aqueous solution under consideration is negative. It is worth mentioning that in the recent work,[49] on the basis of *ab initio* molecular dynamics, a positive value of the surface potential of water was obtained. The contradiction with the data from the partial charge model of water[45,46,48] was explained by the need of taking into account the spatial charge distribution in the water molecule rather than using the effective point-charge model. It seems to be very important to apply *ab initio* molecular dynamics to the calculation of the local electric potential at the interface between an electrolyte solution and a surfactant in order to compare the results with those produced by classical MD simulations.

If the potential is measured from its value in the bulk region, it takes the form of a short-range function concentrated inside the micellar crown with a steep increase to values near zero and then rapidly fading oscillations (curve 1 in Figure 7a). The positive value of the potential near the hydrophobic core of the anionic micelle is caused by water molecules. Curve 2 in Figure 7a corresponds to the same micelle in a continuous solvent with a constant dielectric permittivity of 78.5. The monotonic behavior of the potential in this case could be described by the PB approximation, in contrast to the system with explicit water (curve 1).

These conclusions do not depend on the water model and on the choice of the model parameters. It is obvious that the compensating contribution of water stems from the spatial separation of partial charges in water molecule and not from specific parameters of the water model. The notion of charge separation in water molecule is employed to reproduce appropriately the molecular dipoles and hydrogen bonding of water. So, it seems to be a natural and quite well-founded idea. Apart from this, the advantage of the SPC/E model is that the model gives quite reasonable values for the dielectric permittivity of the bulk water as well as for mobility of ions in electrolyte solutions. Nevertheless, the recent *ab initio* molecular dynamics results[49] for the surface potential of water raise new questions on the need of an additional justification of using partial charge models for any polar substances.

Figure 7b shows the local electric potentials for systems with anionic and cationic micelles. Both functions approach rapidly the zero value in the "bulk" region. At the external boundary, the potentials in both systems are characterized by the same value of the potential difference between liquid and vapor phases. This supports the conclusion about the absence of the counterion influence on the local electric potential at a long distance from the micelle.

IV. CONCLUSIONS

Thus, the results obtained in MD simulations of micelles with explicit water allow us to conclude that the contribution of water plays the main role in determining the behavior of local electric potential, practically compensating for the contribution of counterions at middle and long distances from the micelle. This agrees with a substantial contribution of water to local charge distribution near metal surfaces.[23−29] That means that around the spherical micelles there is no diffuse charged layer usually supposed as a part of the EDL. This coincides with conclusions about a multilayer structure of solvent with ions obtained on the basis of the integral equations.[50] A natural consequence of this fact is a short-range dependence of the electric field on the distance from the micelle. The same results

dx.doi.org/10.1021/jp3024183 | J. Phys. Chem. B 2012, 116, 5795−5800

can be obtained for any spherical macroions and biopolymer systems.[51] So, as opposed to a commonly used notion, the electric field of ionic micelles with a water contribution is short-ranged, even without salts in the solution. Obviously, the use of mean-field theories to describe the local potential in these systems faces serious difficulties, and questions can be raised about limitations of the DLVO theory when a correct description of colloidal solutions is needed.

As it was said above, similar results could be obtained with any partial charge model of water and should not depend on the choice of the model parameters. These water models were widely and successfully used for various aqueous systems including electrolyte solutions. However, a striking disagreement was found[49] between the values of surface potential of pure water obtained by classical and *ab initio* molecular dynamics. This calls in question the use of the well-known water models for description of various aqueous solutions. It would be very important to investigate the whole set of water properties including dielectric permittivity and ability for hydrogen bond formation using *ab initio* molecular dynamics. At present, it is difficult to predict how the conclusions about local electric properties of a surfactant interface could change when *ab initio* molecular dynamics is used instead of classical approaches.

AUTHOR INFORMATION

Notes

The authors declare no competing financial interest.

ACKNOWLEDGMENTS

The work was supported by the scientific research plan of the Saint Petersburg State University (No. 12.37.127.2011) and by the Federal Support Program for Scientific Schools (NSh-4464.2012.03).

REFERENCES

(1) Lyklema, J. *Fundamental of Interface and Colloid Science*; Academic Press: London, 1995; Vol. *2*, 779 pp.
(2) Allen, M. P.; Tildesley, D. J. *Computer Simulation of Liquids*; Oxford University Press: New York, 1989; 385 pp.
(3) Frenkel, D.; Smit, B. *Understanding Molecular Simulation: From Algorithms to Applications*; Academic Press: New York, 2002; 638 pp.
(4) Torrie, G. M.; Valleau, J. P. *J. Chem. Phys.* **1980**, *73*, 5807−5816.
(5) Torrie, G. M.; Valleau, J. P.; Patey, G. N. *J. Chem. Phys.* **1982**, *76*, 4615−4622.
(6) Valleau, J. P.; Torrie, G. M. *J. Chem. Phys.* **1984**, *81*, 6291−6295.
(7) Torrie, G. M.; Valleau, J. P.; Outhwaite, C. W. *J. Chem. Phys.* **1984**, *81*, 6296−6300.
(8) Carnie, S. L.; Torrie, G. M. *Adv. Chem. Phys.* **1984**, *56*, 141−253.
(9) Boda, D.; Henderson, D.; Chan, K.-Y. *J. Chem. Phys.* **1999**, *110*, 5346−5350.
(10) Boda, D.; Henderson, D.; Chan, K.-Y.; Wasan, D. T. *Chem. Phys. Lett.* **1999**, *308*, 473−478.
(11) Boda, D.; Fawcett, W. R.; Henderson, D.; Sokołowski, S. *J. Chem. Phys.* **2002**, *116*, 717012.
(12) Boda, D.; Henderson, D.; Plaschko, P.; Fawcett, W. R. *Mol. Simul.* **2004**, *30*, 137−141.
(13) Outhwaite, C. W. *J. Chem. Soc., Faraday Trans. 2* **1986**, *82*, 789−794.
(14) Bhuiyan, L. B.; Outhwaite, C. W. *Philos. Mag. B* **1994**, *69*, 1051−1058.
(15) Hribar, B.; Vlachy, V.; Bhuiyan, L. B; Outhwaite, C. W. *J. Phys. Chem. B* **2000**, *104*, 11522−11527.
(16) Outhwaite, C. W.; Bhuiyan, L. B. *Electrochim. Acta* **1991**, *36*, 1747−1749; *Mol. Phys.* **1991**, *74*, 367−381.
(17) Degreve, L.; Lozada-Cassou, M.; Sanchez, E.; Gonzfilez-Tovar, E. *J. Chem. Phys.* **1993**, *98*, 8905−8909.
(18) Degreve, L.; Lozada-Cassou, M. *Mol. Phys.* **1995**, *86*, 759−768.
(19) Lamperski, S.; Bhuiyan, L. B. *J. Electroanal. Chem.* **2003**, *540*, 79−87.
(20) van der Maarel, J. R. C. *Biophys. J.* **1999**, *76*, 2673−2678.
(21) Boda, D.; Henderson, D. *J. Chem. Phys.* **2000**, *112*, 8934−8938.
(22) Semashko, O. V.; Burov, S. V.; Brodskaya, E. N. *Colloid J.* **2009**, *71*, 846−851.
(23) Glosli, J. N.; Philpott, M. R. *Electrochim. Acta* **1996**, *41*, 2145−2158.
(24) Halley, J. W.; Mazzolo, A.; Zhou, Y.; Price, D. *J. Electroanal. Chem.* **1998**, *450*, 273−280.
(25) Spohr, E. *Electrochim. Acta* **1999**, *44*, 1697−1705.
(26) Crozier, P. S.; Rowley, R. L. *J. Chem. Phys.* **2000**, *113*, 9202−9205.
(27) Dimitrov, D. I.; Raev, N. D. *J. Electroanal. Chem.* **2000**, *486*, 1−8.
(28) Oyen, E.; Hentsche, R. *Langmuir* **2002**, *18*, 547−556.
(29) Guymon, C. G.; Hunsaker, M. L.; Harb, J. N.; Henderson, D.; Rowley, R. L. *J. Chem. Phys.* **2003**, *118*, 10195−10202.
(30) Schweighofer, K. J.; Essmann, U.; Berkowitz, M. *J. Phys. Chem. B* **1997**, *101*, 10775−10780.
(31) Shelley, J. C.; Shelley, M. Y. *Curr. Opin. Colloid Interface Sci.* **2000**, *5*, 101−110.
(32) Brodskaya, E. N. *Colloid J.* **2012**, *74*, 154−171.
(33) Rakitin, A. R.; Pack, G. R. *Colloids Surf., A* **2003**, *218*, 265−276.
(34) Rakitin, A. R.; Pack, G. R. *J. Phys. Chem. B* **2004**, *108*, 2712−2716.
(35) Tieleman, D. P.; van der Spoel, D.; Berendsen, H. J. C. *J. Phys. Chem. B* **2000**, *104*, 6380−6388.
(36) Lubartsev, A. P. Molecular Simulations of DANN Counterion Distributions. *Dekker Encyclopedia of Nanoscience and Nanotechnology*; 2004; pp 2131−2142.
(37) Berendsen, H. J. C.; Grigera, J. R.; Straatsma, T. P. *J. Phys. Chem.* **1987**, *91*, 6269−6271.
(38) Mohanty, S.; Davis, H. T.; McCormick, A. V. *Langmuir* **2001**, *17*, 7160−7171.
(39) Dang, L. X. *J. Am. Chem. Soc.* **1995**, *117*, 6954−6960.
(40) Jorgensen, W. L.; Madura, J. D.; Swenson, C. J. *J. Am. Chem. Soc.* **1984**, *106*, 6638−6646.
(41) Bruce, C. D.; Berkowitz, M. L.; Perera, L.; Forbes, M. D. E. *J. Phys. Chem. B* **2002**, *106*, 3788−3793 , 10902−10907.
(42) Yoshii, N.; Iwahashi, K.; Okazaki, S. *J. Chem. Phys.* **2006**, *124*, 184901.
(43) Yoshii, N.; Iwahashi, K.; Okazaki, S. *J. Chem. Phys.* **2007**, *126*, 096101.
(44) Jorge, M. *Langmuir* **2008**, *24*, 5714−5725.
(45) Zakharov, V. V.; Brodskaya, E. N. *J. Chem. Phys.* **1995**, *102*, 4595−4599.
(46) Zakharov, V. V.; Brodskaya, E. N.; Laaksonen, A. *J. Chem. Phys.* **1997**, *107*, 10676−10683.
(47) Zakharov, V. V.; Brodskaya, E. N.; Laaksonen, A. *Mol. Phys.* **1998**, *95*, 203−209.
(48) Wilson, M. A.; Pohorille, A.; Pratt, L. R. *J. Chem. Phys.* **1988**, *88*, 3281−3285.
(49) Kathmann, Sh. M.; Kuo, I.-F. W.; Mundy, Ch. J.; Schenter, G. K. *J. Phys. Chem. B* **2011**, *115*, 4369−4377.
(50) Howard, J. J.; Perkyns, J. S.; Pettitt, B. M. *J. Phys. Chem. B* **2010**, *114*, 6074−6083.
(51) Tan, C.; Yang, L.; Luo, R. *J. Phys. Chem. B* **2006**, *110*, 18680−18687.